Experimental investigation on crack propagation in Carrara marble subjected to cyclic loading

EXPERIMENTAL INVESTIGATION ON CRACK PROPAGATION IN CARRARA MARBLE SUBMITTED TO CYCLIC LOADS

Maria MIGLIAZZA, Anna Maria FERRERO, Andrea SPAGNOLI
Department of Civil-Environmental Engineering and Architecture
Viale Usberti 181/A, 43100 Parma, Italy

ABSTRACT
In the present paper, the results of an experimental campaign on marble specimens under three- and four-point bending is presented. Firstly static tests on smooth and notched specimens are carried out to determine the tensile strength and the fracture toughness of marble, respectively. Then cyclic tests on smooth and notched specimens are performed to determine the fatigue strength. Moreover, in the case of notched specimens where an indirect measure of the crack length is performed, the results of cyclic tests allow the determination of the fatigue growth rate of cracks. In this way, the material parameters of commonly used fatigue crack growth laws, like the two-parameter law of Paris, can be estimated. This work is part of a wider one which is devoted to the investigation of the mechanical behaviour of marble slabs, used as façade panels to externally cover buildings, under thermal cycles. In particular, some experimental results here presented could be used to simulate by means of a theoretical model recently presented by the authors the evolution of bowing, which is a phenomenon characterised by permanent deflections typically encountered in façade panels after a certain time of environmental exposure.

KEYWORDS: bowing, fatigue crack growth, fatigue strength, fracture mechanics, marble.

1. Introduction

Carrara marble is frequently used as façade panels to externally cover buildings. These panels are subjected to different actions that deteriorate the material, including: temperature (daily and seasonal excursions, through-thickness gradient), mechanical loads (wind, self-weight), chemical attacks (acid rain), humidity changes. Temperature may induce stresses due to thermal expansion (restraint effects of the anchorage system, nonlinear temperature fields, nonuniform thermal expansion). One visible phenomenon connected to deterioration of marble is bowing, which is characterised by permanent out-of-plane deflections. Bowing is generally accompanied by an overall reduction of strength which increases with increasing degree of bowing, while at the microstructural level of the material bowing is

accompanied by a decohesion of calcite grains.

In order to understand the phenomenon of bowing in marble slabs, several experimental and theoretical studies [1-7] have been carried out, starting with the pioneering work of Rayleigh in 1934 [8]. The results of these studies show that the strength of marble after environmental exposition decreases due to grain decohesion. In particular, Royer [4] showed that thermal action produces self-equilibrated stress states at calcite grain (whose size ranges typically between 100 and 500 μm) interfaces, which are responsible of progressive damage in the material leading to initiation and propagation of intergranular cracks. As a matter of fact calcite grains present an anisotropic thermal expansion. More precisely there exists a maximum thermal expansion along the optic axis of the grain and a minimum thermal expansion normal to it (the thermal expansion coefficient turns out to be negative along this axis) [8].

The determination of the overall mechanical behaviour of marble slabs on the basis of the aforementioned micromechanical phenomena might be performed within the framework of Linear Elastic Fracture Mechanics (LEFM) (e.g. see Ref. [9]). Accordingly, stress/strain state induced by cyclic thermal loading acting on the marble slab can be determined along with the deflection (bowing) of the slab due to both elastic bulk deformation and intergranular cracks. As the cracks propagate under cyclic thermal loading, the level of bowing after a certain number of thermal cycles and the fatigue life (expressed in terms of number of thermal cycles causing the collapse of the slab) can be calculated.

The present authors have recently proposed in Refs [10, 11] a theoretical model to estimate the progressive bowing and the thermal fatigue of marble slabs submitted to temperature cycles is presented. The model, developed within the framework of LEFM, takes into account the mechanical microstructural characteristics of the marble as well as the actual cyclic temperature field in the material. The slabs are subjected to a thermal gradient along their thickness (due to different values of temperature between the outer and inner sides of the slab) as well as to thermal fluctuation on the two sides of the slab due to daily and seasonal temperature excursions. This thermal action causes a stress field which can locally determine microcracks due to decohesion of grains. Stress intensification near the cracks occurs and leads to crack

propagation in the slab. Such crack propagation under thermal actions is evaluated and the corresponding deflection (bowing) is calculated.

In the present paper, the results of some static and cyclic experimental tests on Carrara marble are presented. The aim of the research is twofold: (i) evaluate the fatigue strength; (ii) estimate the fatigue crack growth rate.

2. Experimental set-up and tested material

An experimental campaign is carried out by performing a series of tests on smooth and notched specimens submitted to static and cyclic loading. The specimens were taken from the marble claddings of a building in Pescara (Italy) where bowing phenomena were experienced [10]. Tests are performed at the Department of Civil-Environmental Engineering and Architecture of the University of Parma and at the commercial laboratory Marmotest in Carrara.

Specimens have a prismatic shape with the following dimensions: length L = 22 cm, span S = 12 cm, height W = 6 cm and width B = 3 cm. Notched specimens are characterized by a central edge notch machined by means of a water jet technique. Notches with different nominal dimensions are machined, so that the notch depth is equal to 3, 6 and 9 mm (the notch width is kept equal to 1.5 mm due to some technical constraints). Both smooth and notched bars are tested under three and four point bending conditions (Figure 1). For the latter condition the distance D between loads is equal to 60 mm (D = S/3).

The static tests on smooth specimens allow us to determine the tensile resistance T_o of marble, while their counterparts on notched specimens allow us to determine the failure load P_u and the critical stress intensity factor (fracture toughness) K_{Ic}. On the other hand by performing fatigue tests the number of cycles to failure (fatigue life) and the fatigue crack growth rate is investigated on smooth specimens and notched specimens, respectively.

The material under study is analyzed with a binocular Zeiss-Axiolab microscope with ocular E-PL 10x/20 and lens plan-NEOFLUAR 2.5x/0.075, ACHROPLAN 10x70.25 on four thin sections (Figure 2). Results of the petrography analysis show that the

marble is a compact and homogeneous rock with metamorphic origin, mostly made of carbonate with calcite crystal of sub-millimetre dimensions. The material does not show the presence of open or cemented cracks or of alteration phenomena. The microstructure is granoblastic, polygonal and mainly equigranular. The marble is made of calcite crystals characterized by triple contact points at 120° among them. Crystal average dimension varies between 180 ± 50 μm and 220 ± 50 μm. No preferential crystal orientations are observed.

Standard parameters of the mechanical characteristics in terms of resistance and deformability were previously determined at the National Research Council Laboratory of Politecnico di Torino on the same material [12]. These parameters are reported in Table 1 where E is the elastic modulus, ν is the Poisson ratio, C_o is the compressive strength, T_o is the tensile strength, c and ϕ are the cohesion and the friction angle respectively used in the Mohr-Coulomb failure criterion.

2.1 Results of static tests

Ten static tests are performed on smooth specimen under four point bending. Load-controlled tests with a load rate equal to 160 N/s. During testing, both the applied load and vertical displacements using two LVDT sensors are acquired with a frequency of 100 Hz. Table 2 reports the results of the tests where the reported value of the tensile strength is calculated according to classical beam theory.

Six fracture toughness tests on notched specimens with notch depth a_0 = 6 mm under three-point bending are performed according to the Two Parameter Model (TPM) [13]. This model allows the computation of two fracture parameters which are unaffected by scale effects: the critical stress intensity factor (K_{Ic}) and the critical Crack Tip Opening Displacement ($CTOD_c$).

Tests are performed by means of a servo-hydraulic actuator INSTRON 8862 which allows the application of load under a constant crack opening rate. In this way, the complete load-crack opening curve can be recorded even in the post-peak (softening) phase. Crack mouth opening displacement (CMOD) is recorded by means of a clip gauge (Figure 3). The CMOD rate is kept as low as 1μm/min during the tests.

In order to determine the critical stress intensity factor [13], specimens are unloaded just after the peak load. Accordingly, five tests on notched specimens are performed under an initial load rate control followed by a CMOD rate control up to a load, in the post-peak stage, which is 85-95% of the peak load. During unloading-reloading the tests are performed under load rate control.

From the load-CMOD curve the initial slope and the secant unloading-reloading line can be drawn, and, hence, the initial compliance C_i and the ultimate (namely, related to the peak load) compliance C_u can be worked out.

Figure 3 shows two examples of load–CMOD curves along with the lines drawn to determine the initial and ultimate compliances. From the determined values of compliances, following the TPM of Ref. [13], the Young modulus (from C_i), the critical crack length, the critical SIF and the critical CMOD (from C_u) can be worked out. The obtained results are reported in Table 4 along the peak load P_u.

2.2 Results of cyclic tests

Two cyclic tests on smooth specimens are performed under four-point bending (Figure 1). Sinusoidal pulsating loads with a frequency in the range 1 to 4 Hz are applied. A maximum load of 77% and 82%, respectively, of the static bending strength (P_u) is applied. The loading ratio R (ratio between minimum and maximum values of the applied load) is equal to 0.05 and 0.06, respectively. The tests show that specimens do not fail (run-out specimens) after 77,000 cycles and 5,000,000 cycles for a load level P_{max}/P_u equal to 82% and 77%, respectively.

Eight cyclic tests on specimens with different initial notch lengths (3 mm, 6 mm and 9 mm, respectively) are performed under four-point bending. These tests are carried out by applying different loading sequences both in terms of frequencies and amplitudes. Frequency is made to vary between 1 and 4 Hz. Some specimens are equipped with a strain-gage glued on the top (compressed) face in the central part of the specimen under constant moment. In this way, the axial compressive strain can be recorded. As the crack depth increases under cyclic loading the measured values of axial compressive strain tend to increase.

All the cyclic tests are performed by means of a servo-hydraulic actuator MTS 810.

3. Fatigue life

Table 5 shows the results obtained from the cyclic tests on both smooth and notched specimens. In particular, initial notch length, minimum and maximum applied load (P_{max} and P_{min}), static failure load P_u, load level P_{max}/P_u, loading rate R ($R = P_{min}/P_{max}$) and the number of cycles to failure are reported. The value of P_u for notched specimens is determined from one static test under four-point bending for each initial notch length. The value of P_u for smooth specimens is the mean value of the results reported in Table 2.

The obtained results are interpreted ia the well-known high-cycle fatigue power law of Basquin (e.g. see Ref. [14]), which describes the experimental S-N relation (Wohler diagram):

$$P_{\max} = c\, N_f^{-1/k} \tag{1}$$

where c and k are material parameters which can be obtained from a linear fitting of experimental data in the S-N log-log plane (Figure 5).

4. Fatigue crack growth

The evolution curves of the acquired maximum values (during each cycle) of the axial compressive strain is employed to estimate the crack evolution. Figure 6 shows the time history of the maximum axial strain for two tests (D2 and D7).

One can observe that fatigue behaviour of the material is characterised by an initial stage during which crack evolution is very slow (nearly linear phase), whilst crack growth rate increases during a final stage as failure is approached.

The observed variation of axial strain indicates a reduction of the ligament height as a consequence of fatigue crack propagation. Hence, an indirect measure of crack depth, and, hence, of fatigue crack growth rate can be performed from the axial strain on the top face of the specimen.

In order to correlate strain and crack depth a linear elastic two-dimensional FE model is built up. In the model the actual loading and geometric conditions of the specimens are simulated (Figure 7). Due to symmetry conditions only a half of the specimens is modelled. A fine mesh with 21901 nodes and 21600 4-node plane stress elements is generated. Young modulus is equal to 50 GPa and Poisson ratio to 0.15. A unit total load is applied to the FE model under four-point bending.

A series of linear analysis under the unit load is carried out, where in each analysis the height of the ligament is reduced by releasing, node by node, the symmetry boundary conditions along the mid-span cracked section (a crack depth up to 40mm with a crack depth step of 0.5mm is simulated). For each crack configuration the axial strain on the top face of the FE model is picked up. The relation between crack depth and axial strain is shown in Figure 8.

The obtained curve is calibrated for each experimental test in order to consider the actual values of strain induced by the acting load in the experiments (note that the FE model is run for a unit load). Calibrations are carried out so as to have in the FE models the same deformation ε_0 measured during tests for the known value of the initial crack length. Then a polynomial fitting of the FE results in terms of crack length a vs top face axial strain ε is obtained. In this way, it is possible to correlate the experimentally measured strain to an equivalent crack depth (Figure 8).

The experimental fatigue crack growth results, now expressed (using the aforementioned a-ε relation) in terms of crack length a vs number of loading cycles N, are analysed. In particular the material parameters C and m of the Paris law ($da/dN = C\,\Delta K_I^m$) are estimated [15]. Such a law has been proved to well describe the experimental trend of the fatigue growth of so-called long cracks for a variety of engineering materials with particular regards to metals.

For this purpose, the crack growth rate da/dN versus number of cycles is determined according to ASTM E647 standard [16]. The experimental da/dN-N data are analyzed by an incremental polynomial method. This method for computing da/dN involves fitting a second-order polynomial (parabola) to sets of (2n + 1) successive data points a-N, where n is here taken as equal to 4. The rate of crack growth at each central point a_i, in the range $a_{i-n} - a_{i+n}$, is obtained from the derivative of the above parabola.

The SIF range ΔK_I is determined according to the following LEFM expression (four-point bending for distance between loads D = S/3):

$$\Delta K_I = \frac{PS}{BW^2}\sqrt{\pi a}F(\alpha) \tag{2}$$

where the meaning of the geometrical parameters, S, B and W can be understood from Figure 1, a is the crack length, $P = (1-R)P_{max}$, where R is the loading ratio and F is a geometric parameter function of the relative crack length $\alpha = a/W$ [14].

Figure 9 shows the experimental results in terms of a versus ΔK_I in a log-log plane. The results are interpreted to determine the C and m parameters of the Paris law. Threshold values of crack propagation rate equal to da/dN = 100 μm/cycle (note that the calcite grain size is in the range 100-500 μm) and of ΔK_I = 0.675 $MPam^{0.5}$ (corresponding to 50% of K_{Ic}) are arbitrarily set to exclude the fatigue growth of short cracks from the calculation of Paris law parameters. The relevant results are shown in Figure 10 (in a log-log plane) together with the fitting line from which C and m (slope) parameters can be worked out (Table 6). The obtained results are the first tentative, to the authors' knowledge, to use the Paris law to describe the fatigue growth of cracks in marble elements.

5. CONCLUSIONS

The aim of the present work is to experimentally investigate the fatigue behaviour of marble under cyclic mechanical loading. In particular, the fatigue strength and the fatigue crack growth are investigated. The final goal is to experimentally determine some parameters used in the theoretical model recently proposed by the authors [10, 11] to describe the bowing of marble panels used as cladding elements of building. The mechanical cyclic loads applied in the tests want to somehow reproduce the thermal fluctuations experienced by marble panels during their in-service conditions.

The fatigue strength of smooth and notched specimens is investigated. The obtained results show that on smooth specimens there is a small reduction of strength as compared to the static value (note that the maximum experimentally applied number of loading cycles is 5,000,000 which corresponds to over 10,000 years of daily

thermal cycles).

As far as notched specimens are concerned, fatigue damage is observed since a strength reduction with increasing number of loading cycles is recorded. However, the value of the slope in the S-N log-log curve is equal to -1/30. By extrapolating the obtained data we can notice that for a period of 100 years (equal to 36,500 daily thermal cycles) a slab with an initial defect of 6 mm in length under maximum bending load equal to 35% of the corresponding static strength would not experience a failure. It is important to observe that the notch depth machined in the experimental specimens (3, 6 and 9 mm) is much higher that the defects encountered on naturally damaged marble slab due to grain decohesion. Moreover the applied level of stress in the present experimental fatigue tests is much larger that the thermal stresses induced by daily temperature fluctuations [11].

Finally, tentative values of Paris law parameters are determined from the experimental results concerning the fatigue crack growth in notched specimens. These values represent a first attempt to offer experimental values to describe fatigue damage in marble using LEFM concepts. The findings of the present work might be beneficial when fatigue strength and deformability (bowing) of marble panels submitted to environmental actions (including temperature cycles) are simulated within the framework of LEFM.

REFERENCES

[1] Scheffzuk C, Siegesmund S, Koch A (2004) Strain investigations on calcite marbles using neutron time-of-flight diffraction. *Environmental Geology* Vol. 46, pp. 468-476.

[2] Wong RHC, Chau KT, Wang P (1996) Microcracking and grain size effect in Yuen Long marbles. *International Journal of Rock Mechanics and Mining Science and Geomechanics* Vol. 33, pp. 479-485.

[3] Widhalm C, Tschegg E, Eppensteiner W (1996) Anisotropic thermal expansion causes deformation of marble claddings. *ASCE Journal of Performance of Constructed Facilities* Vol. 10, pp. 5-10.

[4] Royer-Carfagni G (1999) On the thermal degradation of marble. *International Journal of Rock Mechanics and Mining Science* Vol. 36, pp. 119-126.

[5] Leiss B, Weiss T (2000) Fabric anisotropy and its influence on physical weathering of different types of Carrara marbles. *Journal of Structural Geology* Vol. 22, pp. 1737-1745.

[6] Siegesmund S, Ullemeyer K,Weiss T, Tschegg EK (2000) Physical weathering of marbles by anisotropic thermal expansion. *International journal of Earth Sciences* Vol. 89, pp. 170-182.

[7] Ferrero AM, Marini P (2001) Experimental studies on the mechanical behaviour of two thermal cracked marbles. *Rock Mechanics and Rock Engineering* Vol. 34, pp. 57-66.

[8] Raileigh A (1934) The bending of marble. *Proceeding Royal Society of London* Vol. 19, pp. 266-279.

[9] Chau KT, Shao JF (2006) Subcritical crack growth of edge and center cracks in façade rock panels subject to periodic surface temperature variations. *International Journal of Solids and Structures* Vol. 43, pp. 807-827.

[10] Ferrero AM, Migliazza M, Spagnoli A (2009) Theoretical modelling of bowing in cracked marble slabs under cyclic thermal loading. *Construction and Building Material* Vol. 23, pp. 2151-2159.

[11] Spagnoli A, Ferrero AM, Migliazza M (2010) A micromechanical model to describe thermal fatigue and bowing of marble. *Fatigue & Fracture of Engineering Materials & Structures* (submitted).

[12] CNR-IGAG (2007). Risultati di prove sperimentali condotte sul marmo bianco di Carrara (*in Italian)*. Private communication.

[13] Jenq Y, Shah SP (1985). Two parameter fracture model for concrete. *ASCE Journal of Engineering Mechanics*, Vol. 111, pp. 1227-1241.

[14] Suresh S. (1998) *Fatigue of Materials*. Cambridge University Press, Cambridge.

[15] Paris PC, Erdogan F (1963). A critical analysis of crack propagation laws. *Journal of Basic Engineering*, Vol. 85, pp. 528-534.

[16] ASTM E647-08. *Standard Test Method for Measurement of Fatigue Crack Growth Rates.*

Table 1. Mechanical parameters of the tested marble [12]

Compressive strength C_o [MPa]		89.7
Tensile strength T_o [MPa]		8.97
Elastic modulus	secant E_s [GPa]	52.45
	tangent E_t [GPa]	75.42
Poisson ratio	secant ν_s	0.16
	tangent ν_t	0.30
Mohr-Coulomb failure criterion	cohesion c [MPa]	20.70
	friction angle ϕ [°]	38.4

Table 2. Four-point bending results for smooth specimens

	Failure load	Maximum mid-span deflection			Tensile strength		
specimen	P_u [kN]	s_{MAX} [mm]	Mean	SD	T_0 [MPa]	Mean	SD
Cs1	9.39	0.175			15.9		
Cs2	8.89	0.195			14.7		
Cs3	10.42	0.162	0.185	0.04	17.4	16.9	3.08
Cs4	8.59	0.150			14.4		
Cs5	13.57	0.244			22.0		
Es1	8.16	0.174			12.7		
Es2	8.95	0.155			13.9		
Es3	8.66	0.176	0.171	0.01	13.4	13.0	0.75
Es4	8.23	0.168			12.7		
Es5	7.72	0.179			12.0		

Table 3. Load and CMOD at peak condition; initial (C_i) and final (C_u) compliances obtained from the load-CMOD curves

specimen	Peak condition		Compliance	
	load [kN]	CMOD [10^{-3}mm]	C_i [m/kN]	C_u [m/kN]
E0	3.04	11.67	1.75E-06	3.51E-06
E1	2.96	17.46	2.78E-06	5.79E-06
E2	3.00	13.68	2.65E-06	5.16E-06
C1	2.84	5.04	1.88E-06	2.89E-06
C2	2.98	7.12	2.12E-06	2.42E-06
C3	2.73	5.74	1.64E-06	2.75E-06
Mean	2.92	10.12	2.14E-06	3.75E-06
SD	0.12	4.96	4.77E-07	1.39E-06

Table 4. Estimated values of elastic modulus E, critical crack length a_c*, critical stress intensity value* K_{Ic} *and critical crack tip opening displacement (*$CTOD_C$*)*

Specimen	E [GPa]	a_c [mm]	K_{Ic} [$MPam^{1/2}$]	$CTOD_C$ [10^{-3}mm]
E0	44.60	11.42	1.32	6.94
E1	28.81	12.02	1.32	11.27
E2	31.12	11.69	1.31	9.86
C1	50.08	10.08	1.23	4.44
C2	42.58	7.45	1.12	2.40
C3	85.30	10.70	1.79	4.18
Mean	47.08	10.56	1.35	6.52
SD	20.42	1.68	0.23	3.48

Table 5. Cyclic test results on smooth and notched specimens

specimen		initial notch length a_o	P_u	P_{max}	P_{max}/P_u	P_{min}	Loading ratio R	Cycles to failure N_f
		[mm]	[kN]	[kN]	[%]	[kN]		
Smooth	I1	0	9.26	7.20	77	0.40	0.06	> 76988
	I2			7.60	82	0.50	0.07	> 5063000
Notched	D1	3	5.63	3.73	66	0.45	0.12	150
	D2			3.75	66	0.50	0.13	2830
	D3			3.10	55	0.30	0.10	> 518400
	D4	6	4.54	2.60	57	0.26	0.10	629850
	D5			3.10	68	0.31	0.10	264100
	D6			3.60	79	0.36	0.10	425
	D7	9	3.2	3.04	95	0.54	0.18	2200
	D8			2.54	79	0.23	0.09	871913

Table 6. Experimentally estimated parameters of the Paris law

specimen	lnC	C	m
D2	-7.90	0.00037	4.37
D7	-8.52	0.00020	3.42
Mean	-8.1	0.00030	3.84

Figure

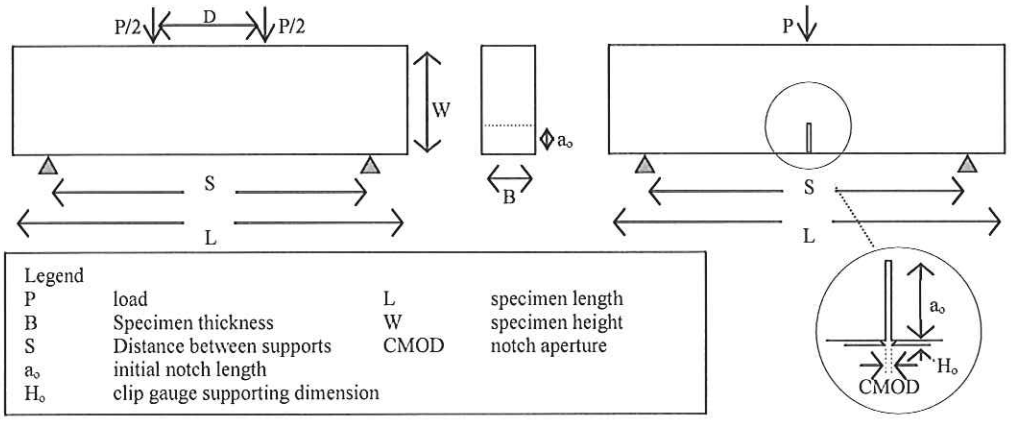

Legend			
P	load	L	specimen length
B	Specimen thickness	W	specimen height
S	Distance between supports	CMOD	notch aperture
a_o	initial notch length		
H_o	clip gauge supporting dimension		

Figure 1. Geometry and loading scheme of three and four point bending tests.

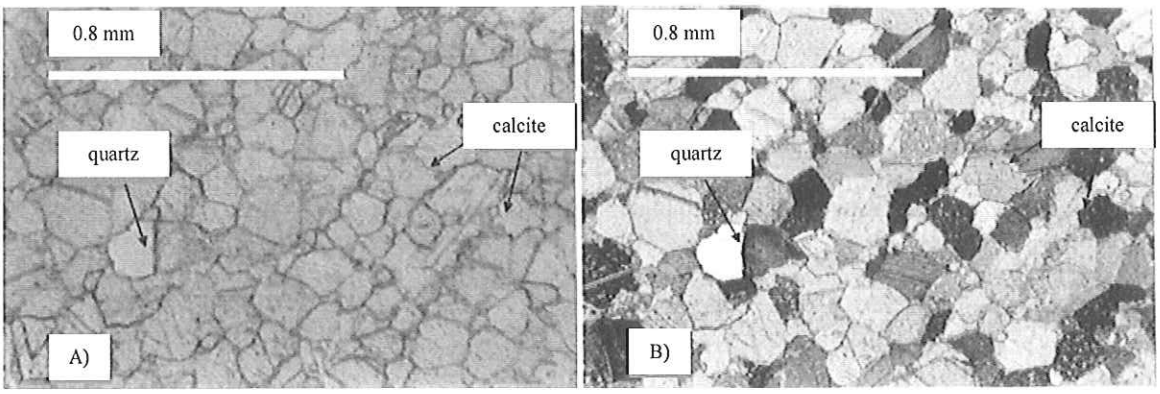

Figure 2. Marble microstructure observed by the thin sections; a) parallel nicol; b) crossed nicol.

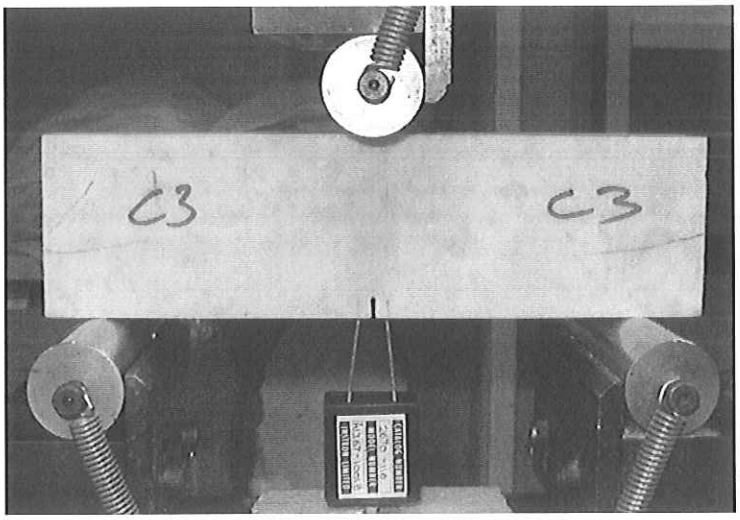

Figure 3. View of a three point bending set up used for static tests.

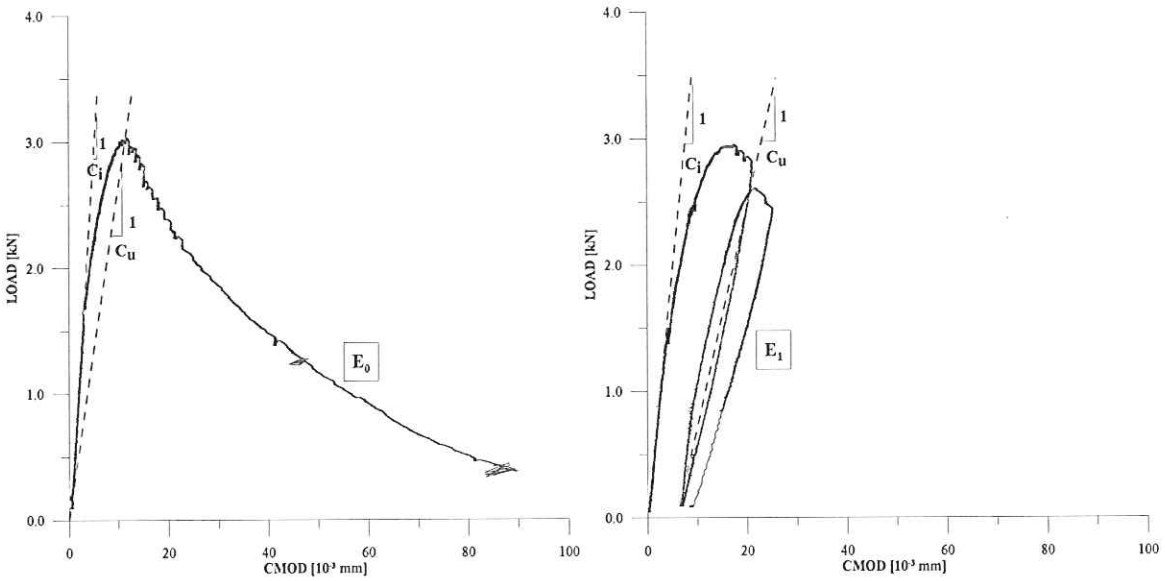

Figure 4. Load – CMOD curves for two notched specimens.

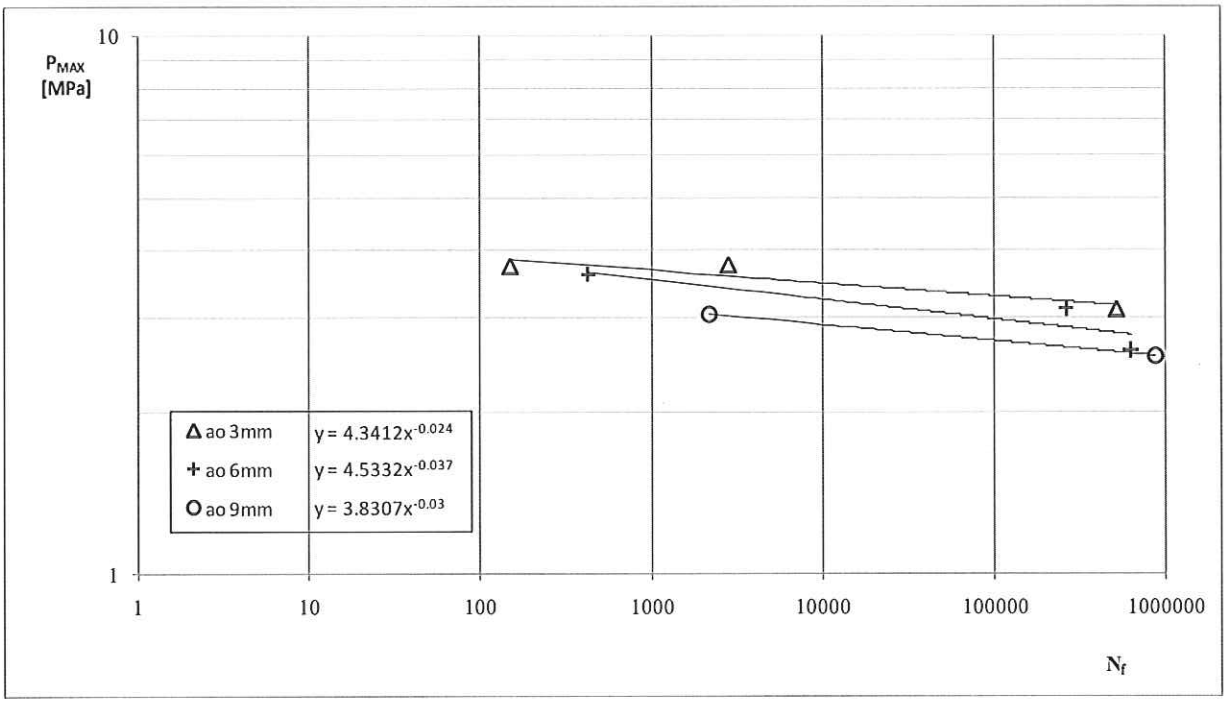

Figure 5. Wohler curves in terms of maximum load P_{max} versus number of cycles to failure N_f for notched specimens

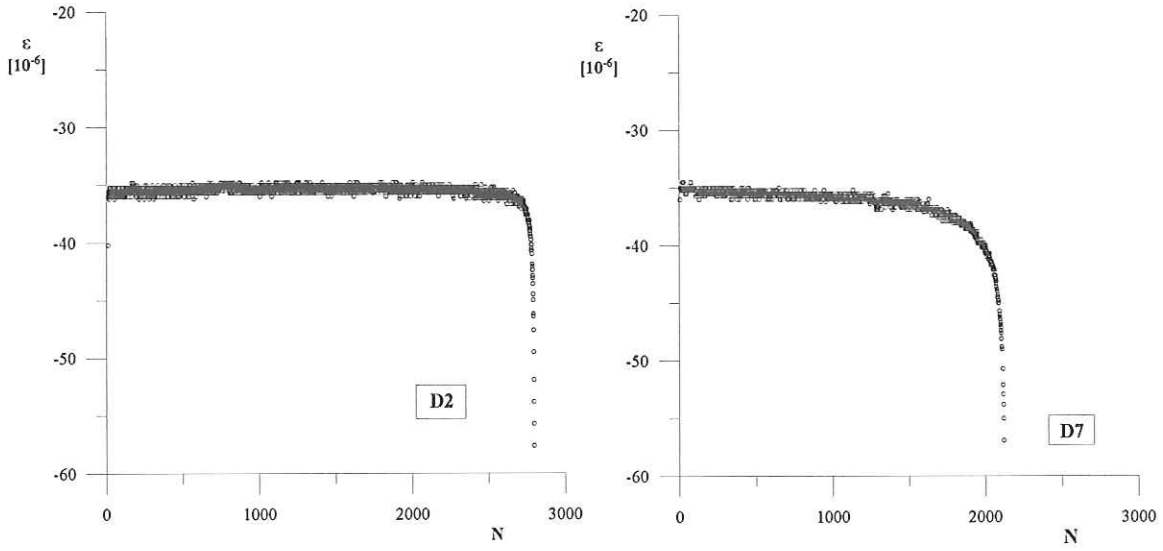

Figure 6. Maximum values of axial compressive strain per cycle against number of loading cycles for the notched specimens D2 and D7.

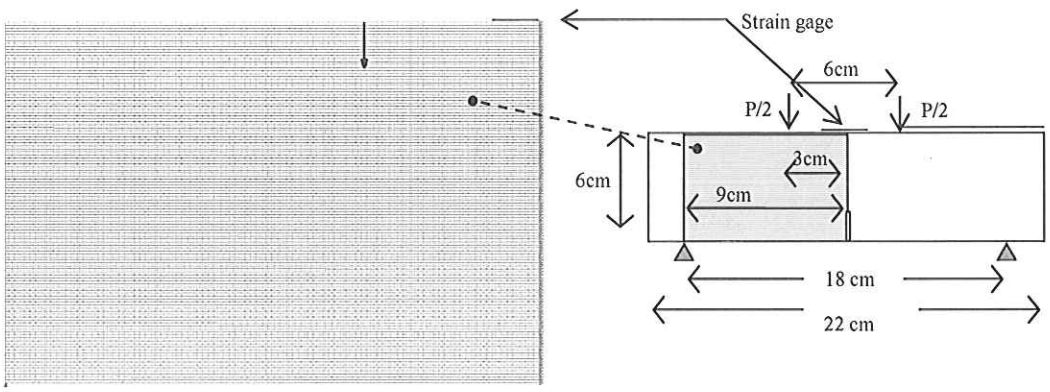

Figure 7. FEM model

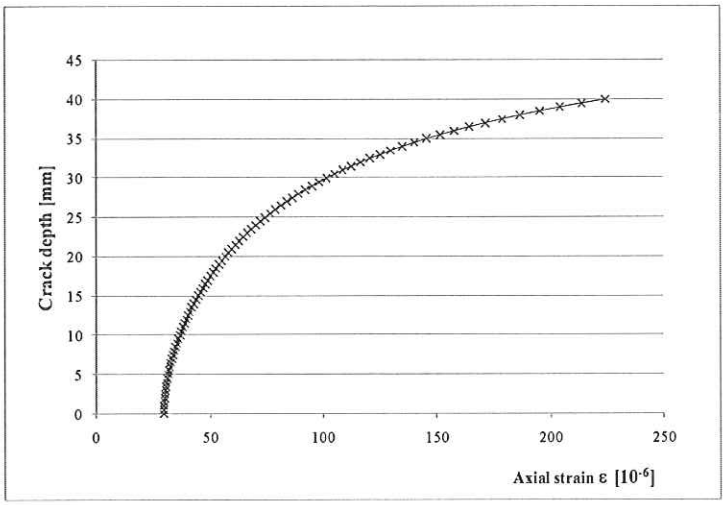

Figure 8. Crack depth against axial strain curves obtained according to FEM analysis.

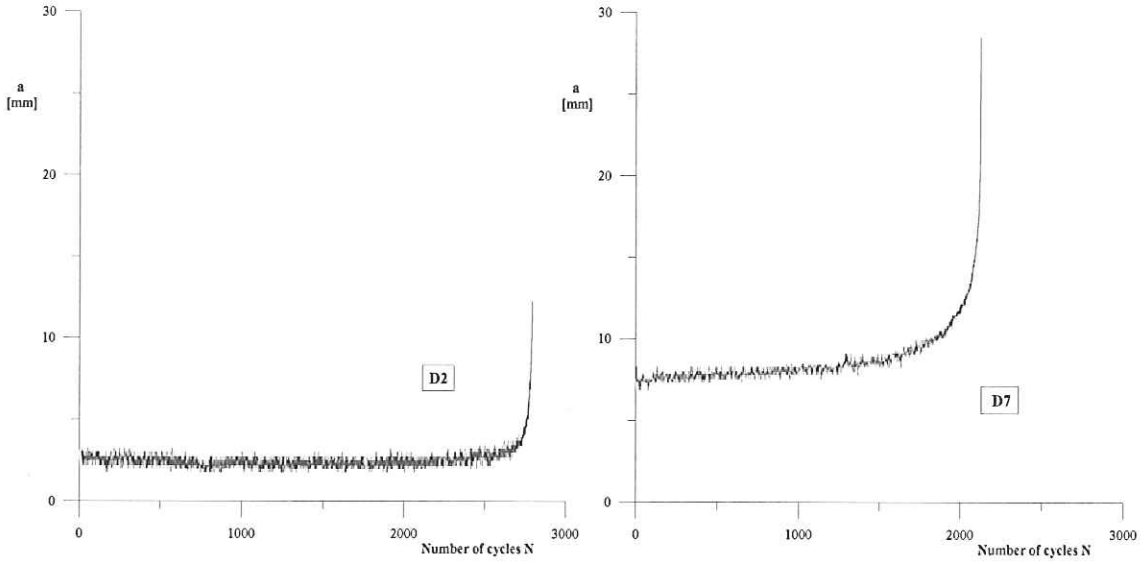

Figure 9. Estimated crack depth against number of cycles for notched specimens D2 and D7.

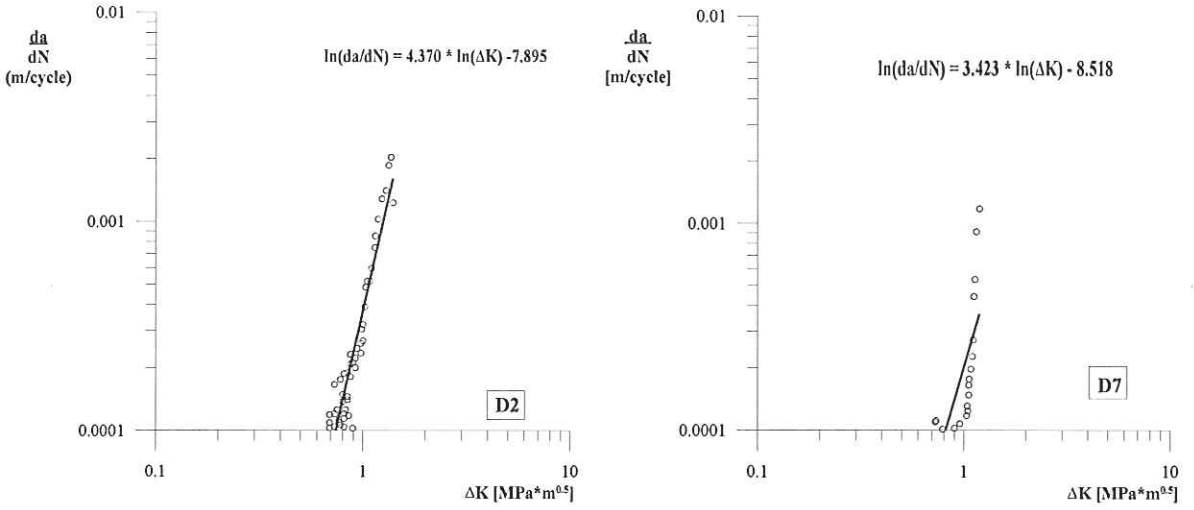

Figure 10. Experimental results obtained in terms of da/dN versus □K for notched specimens D2 and D7.